IEEE Access
Multidisciplinary | Rapid Review | Open Access Journal

Received September 18, 2019, accepted October 24, 2019, date of publication November 4, 2019,
date of current version November 18, 2019.

Digital Object Identifier 10.1109/ACCESS.2019.2951490

A Measurement-Division Model for TDOA-Based Source Bearing Estimation With Unknown Propagation Speed

XUNXUE CUI[1], KEGEN YU[2], (Senior Member, IEEE), AND BAITING ZHAO[1]
[1]School of Electrical and Information Engineering, Anhui University of Science and Technology, Huainan 232001, China
[2]School of Environmental Science and Spatial Informatics, China University of Mining and Technology, Xuzhou 221116, China

Corresponding authors: Xunxue Cui (xxcui@tsinghua.org.cn) and Kegen Yu (kegen.yu@foxmail.com)

This work was supported in part by the National Natural Science Foundation of China under Grant 41574031 and Grant 41730109.

ABSTRACT This paper focuses on the bearing estimation problem of far-field signal source via time-difference-of-arrival (TDOA) with a synchronized array in 3-D space. It is usually assumed that the propagation speed (PS) is perfectly known in localization. In reality, only an imperfect knowledge of PS could be obtained. The traditional closed-form solutions without involving PS have the advantage of low complexity, but suffer from low estimation accuracy. A measurement-division model is proposed to offer an alternative solution without the need of the propagation speed. This speed-free model combines two original TDOA measurement equations into a division formula, whose Cramer-Rao lower bound (CRLB) is derived for the observed data. A typical optimization method, i.e. the Levenberg-Marquardt (LM) algorithm is adopted to resolve the nonlinear measurement-division model, resulting in an estimation accuracy improvement because of its iterative search behavior. The theoretical performance of this solution is evaluated in terms of bias and covariance. Simulations are conducted to demonstrate an accuracy advantage of the solution over the related methods.

INDEX TERMS Bearing estimation, Levenberg-Marquardt, measurement-division, propagation speed, sensor array, speed-free, time-difference-of-arrival.

I. INTRODUCTION

Recently the source bearing estimation problem has been of considerable interest, particularly in Internet of Things and gunshot localization [1]. The source signal enables a point positioning if it is a spherical wave; however, it is only applicable to estimating the source direction if it is a plane wave from a far-field source [2]. A far-field source is not necessarily far away from a sensor array. Usually this source has a very small ratio of array aperture to the distance between array and source, such that its signal wave becomes linear with negligible curvature and can be treated as a plane wave. A typical case is the short baseline array mounted on a vehicle for determining the bearing of gunshot [3].

Direction estimation is also known as direction-of-arrival (DOA) or angle-of-arrival estimation for plane wave in the literature of signal processing. To estimate passively the bearing of an uncooperative source, TDOA measurements are typically exploited, which is measured by the received signals at different sensors of a synchronized array.

Many high resolution algorithms have long been used for DOA estimation in frequency domain, such as MUSIC, ESPRIT and the variants of them [4], [5]. Compressive sensing based methods are novel DOA estimators with high resolution, and work efficiently in 3-D space even using one snapshot [6]. As [7] has pointed out, DOA estimators based on spatial spectral estimation could provide a superior performance over TDOA-based methods due to the combination of the various sensor pairs.

In contrast to those spatial spectral beamformers, the TDOA-based DOA estimators may not perform as well as them in estimation accuracy, but can execute data processing with a low computational complexity in time domain. It is especially suited for the source with a transient and peak signal wave. In this case, the spectral structure of signal is often unknown, and only the arrival difference of pulse time at different sensors can be measured.

The associate editor coordinating the review of this manuscript and approving it for publication was Taufik Abrao.

TDOA-based techniques mostly depend on the assumption that the propagation speed (PS) of a source signal is given as a constant. This hypothesis allows establishing a relation between the range difference and the related TDOA. For example, a known PS can work in the following scenarios:

1) The travel speed of a signal wave is fixed and not subject to appreciable environmental influence, e.g. the PS of electromagnetic wave in the earth's lower atmosphere is normally assumed to be 3×10^8 m/s, namely the speed of light. 2) The environmental condition of signal propagation can be controlled, such as in the acoustic indoor localization when the room temperature is not varied and there is no strong wind-blowing [8]. 3) The physical parameters of propagation medium may be obtained by measurement devices, such as meteorological parameters of field area [9], and seismic factors of solid medium [10], then the PS is calculated using those data. Given a PS value, the TDOA measurements can be exploited to estimate the position or bearing of a source.

However, the PS parameter is usually non-constant [11] [12]. Because the propagation environments are sometimes dynamic and unpredictable, so that the assumption of constant PS is questionable. One such scenario is gunshot and artillery bomb localization, where a long range of acoustic propagation suffers from temperature, wind speed, wind direction and humidity, as well as sound scattering generated by forests, mountains and lakes [13]. Another representative case is the underwater sonar localization, where the PS varies with depth, temperature, and salinity. Third example is that the physical characteristics of non-uniform solid medium may exhibit a high variability, greatly influencing the propagation of seismic wave.

Consequently, TDOA can be converted into range difference only when the PS parameter is perfectly known or an accurate estimate is available [14]. Otherwise, those source localization techniques based upon the range difference are not applicable. In cases where the PS is unknown, uncertain, or inexact, it is referred to as nuisance variable that is no of direct interest [15], but needs to be taken into account with the parameter(s) to be estimated.

The linearized least-square (LLS) in [16] is a typical speed-free estimator in the closed-form to obtain the source bearing. The closed-form estimator is attractive because it does not have the divergence problem and has a low computational complexity. Nevertheless, it would suffer from low accuracy due to large measurement noise.

Motivated by this consideration, we propose a speed-free and nonlinear model to improve the accuracy of bearing estimation provided that the estimation accuracy is preferred by users. This model adopts a divisional manner, so that a transformed equation is established without the need for the speed parameter. Specifically, the Levenberg-Marquardt (LM) algorithm in nonlinear optimization is used to estimate iteratively the source bearing for the model. The algorithm can interpolate between the Gauss-Newton algorithm and the method of gradient descent [17]. In practice, the bearing estimate from LLS may be undertaken as the first guess in the LM algorithm for iteration.

Of course, other nonlinear optimization techniques such as the quadratically constrained quadratic programming algorithm and even intelligent computation algorithms [9] can also be used to provide a similar estimation performance. As a trade-off between accuracy and computation complexity, the LM algorithm has advantages over other nonlinear optimization algorithms in localization [18].

Since a large variety of electronic devices have high computational capacity nowadays, iterative methods can easily be carried out by these systems. To estimate the source bearing as accurately as possible, iterative optimization is favored [19]. Moreover, the proposed model and solution are valid to a range of scenarios such as acoustic, sonic, and vibration circumstances.

The contributions of this paper include:

1) A speed-free measurement-division (MD) model is proposed for TDOA-based source bearing estimation; 2) Based on the observed TDOA data, the Cramer-Rao lower bound (CRLB) is derived for our speed-free model, while the CRLB of the original measurement model with an unknown PS is also derived; 3) An optimization solution is developed to resolve the nonlinear MD model, while the theoretical bias and covariance estimated by this solution are analyzed.

The remainder of this paper is organized as follows. In Section II, we briefly present the TDOA-based source bearing estimation problem. A number of estimation methods under the unknown PS are discussed in Section III. In Section IV, the MD model is formulated, following with a derivation of the corresponding CRLB. A solution to resolve this model is given in Section V, and its theoretical performance analysis is also provided. Simulation and evaluation results are presented in Section VI, and conclusions are drawn in Section VII.

II. TDOA-BASED BEARING ESTIMATION PROBLEM

Consider the source bearing estimation of a plane wave impinging on an array as illustrated in Fig. 1. The bearing of a source signal is parameterized by $\boldsymbol{\gamma} = \left[\varphi, \theta\right]^{\mathrm{T}}$, where φ denotes the azimuth, θ represents the elevation, and T is the transpose operator. Let the cap '$\wedge$' over a symbol represent an evaluated or measurement value, while all vectors and matrixes are boldfaced throughout the paper. Moreover, we use E[$*$] to represent an expectation operator.

The unity DOA vector $\mathbf{k}$ of a far-field source is given via a parametrization

$$\mathbf{k} = \begin{bmatrix} \mathrm{k_x} \\ \mathrm{k_y} \\ \mathrm{k_z} \end{bmatrix} = \begin{bmatrix} \cos\theta\cos\varphi \\ \cos\theta\sin\varphi \\ \sin\theta \end{bmatrix} \tag{1}$$

where the three component $\mathrm{k_x}$, $\mathrm{k_y}$ and $\mathrm{k_z}$ are the projections of the unity DOA onto the three coordinate axes.

If the number of array sensors is N, the spatial position of the i-th sensor is labelled as $\mathbf{s}_i = \left[\mathrm{x_i}, \mathrm{y_i}, \mathrm{z_i}\right]$

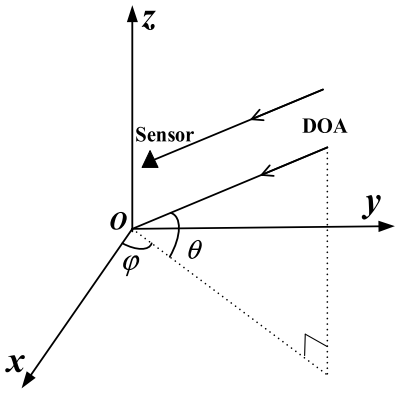

FIGURE 1. Diagram illustrating notation of direction estimation for a far-field signal emitter in 3-D space.

$(\mathrm{i} = 0, 1 \ldots \mathrm{N}-1)$, where $\mathbf{s}_0 = [0, 0, 0]$ is set to be the position of the reference sensor for TDOA measurement. The TDOA between the i-th sensor and the reference sensor is denoted by τ_{i}.

The range difference $\mathrm{c}\tau_{\mathrm{i}}$ is determined by the inner product of the vector $\mathbf{s}_{\mathrm{i}}$ and the DOA vector, where c is the PS parameter of the source signal. That is

$$\tau_{\mathrm{i}} = \mathbf{s}_{\mathrm{i}}\mathbf{k}/\mathrm{c}. \tag{2}$$

If the sensor coordinates except for the reference sensor are aggregated to form a matrix $\mathbf{S} = \left[\mathbf{s}_1^{\mathrm{T}}, \ldots, \mathbf{s}_{N-1}^{\mathrm{T}}\right]^{\mathrm{T}} \in \mathbb{R}^{(N-1)\times 3}$, and so is the set of all TDOAs $\hat{\boldsymbol{\tau}} = \left[\hat{\tau}_1, \ldots, \hat{\tau}_{N-1}\right]^{\mathrm{T}} \in \mathbb{R}^{(N-1)\times 1}$, then traditionally the observation equation of matrix-form is written by

$$\hat{\boldsymbol{\tau}} = \frac{\mathbf{S}\hat{\mathbf{k}}}{\mathrm{c}} + \mathbf{n} \tag{3}$$

where $\mathbf{n}$ is the disturbance vector with component $\{\mathrm{n_i}\}$, $\mathrm{i} = 1, \ldots, N-1$, and $\mathrm{n_i}$ denotes the TDOA measurement error of the i-th sensor.

Assume that $\hat{\boldsymbol{\tau}}$ is a vector of Gaussian noise variables with zero mean and covariance matrix $\boldsymbol{\Sigma}$. In the case of unknown $\boldsymbol{\Sigma}$, we may simply assign it to be [20]

$$\boldsymbol{\Sigma} = \sigma_\tau^2(\mathbf{I} + \mathbf{1}\times\mathbf{1}^T) \tag{4}$$

where σ_τ^2 is the average variance of measurement noise, $\mathbf{I}$ is an identity matrix, and $\mathbf{1}$ is a column vector of ones.

Given the DOA vector estimate in 3-D space, the azimuth/elevation angle of a source is obtained by

$$\begin{cases} \widehat{\varphi} = \tan^{-1}\left(\hat{\mathrm{k}}_{\mathrm{y}}/\hat{\mathrm{k}}_{\mathrm{x}}\right) & \text{(5a)} \\ \hat{\theta} = \tan^{-1}\left(\hat{\mathrm{k}}_{\mathrm{z}}/\sqrt{\hat{\mathrm{k}}_{\mathrm{x}}^2 + \hat{\mathrm{k}}_{\mathrm{y}}^2}\right) & \text{(5b)} \end{cases}$$

Obviously, the angle vector $\boldsymbol{\gamma}$ is the parameter of interest, and yet c is a nuisance parameter in the TDOA-based bearing estimation problem. Note that at the same time this nuisance parameter is a fixed unknown, but it may change at the different measurement moment when we obtain another set of TDOA measurement equations. In the presence of Gaussian variation about the PS, both situations of known and unknown statistical distribution of the PS have been investigated for the time-of-arrival based localization problem in [21], but which is beyond the scope of this paper.

It is worth mentioning that TDOA-based source bearing estimation would be limited to a single source scenario. The spatial spectral beamformers on the other hand can localize more than one source, and even may distinguish between DOAs when the number of signal sources is more than the number of antennas by using compressive sensing [22].

III. RELAED METHODS

Some methods assume that the PS is an unknown variable to be included into the joint estimation for localization of a near-field source through the closed-form manner [23]–[25]. Other methods use the Taylor series least-squares combining with the measurement of environment temperature [8], or employ a bound of PS on a particular occasion to assist the joint estimation [26], [27], such that they comparatively have an accuracy advantage over the closed-form estimators.

When the PS parameter is unknown, it is easy to understand that the joint three-variable (JTV) model in (3) can be used for the source bearing estimation. This model simultaneously estimates PS, azimuth and elevation as a vector of the three unknowns $\boldsymbol{\Theta} = [\varphi\ \theta\ \mathrm{c}]^{\mathrm{T}}$. The three-variable CRLB of the JTV model is derived in Appendix A. As the true CRLB of the original measurement model, the CRLB $(\boldsymbol{\Theta})$ considers the nuisance variable c as part of the estimation problem. The CRLB $(\boldsymbol{\Theta})$ does not bound $\mathrm{E}\left[\left(\hat{\boldsymbol{\gamma}} - \boldsymbol{\gamma}\right)^2\right]$ but $\mathrm{E}\left[\left(\hat{\boldsymbol{\Theta}} - \boldsymbol{\Theta}\right)^2\right]$.

Evidently one feasible method to deal with the PS is adopting the JTV model to estimate the source bearing in our issue. For comparison, the LM algorithm can also be used to resolve the JTV model, whose procedure is provided for reference in Appendix B and called as the JTV solution.

Another feasible method can be considered as an improvement of JTV, which estimates the PS in advance by means of available TDOAs together with sensor coordinates. This scheme is to first determine the PS, and then estimate the remaining source azimuth/elevation.

With regard to the PS estimation of far-field source, [28] has derived an expression under the assumption that a source is far away from the array. Here we propose to estimate the speed parameter, deriving directly from the LLS estimation and the constrained relation among the components of the estimated DOA vector. Specifically, the estimate of LLS is known as

$$\hat{\mathbf{k}} = \mathrm{c}(\mathbf{S}^{\mathrm{T}}\boldsymbol{\Sigma}^{-1}\mathbf{S})^{-1}\mathbf{S}^{\mathrm{T}}\boldsymbol{\Sigma}^{-1}\hat{\boldsymbol{\tau}} \tag{6}$$

subject to a directional quadratic constraint

$$\hat{\mathbf{k}}^{\mathrm{T}}\hat{\mathbf{k}} = 1. \tag{7}$$

This constraint indicates that the ℓ_2-norm of the DOA estimate involving PS should equal one [29]. From the standpoint

of the DOA estimation, we can exactly determine the speed parameter as

$$\hat{c} = \frac{1}{\left\| \left(\mathbf{S}^{\mathrm{T}}\boldsymbol{\Sigma}^{-1}\mathbf{S}\right)^{-1}\mathbf{S}^{\mathrm{T}}\boldsymbol{\Sigma}^{-1}\hat{\boldsymbol{\tau}} \right\|_2}. \tag{8}$$

The estimation accuracy of the PS should be examined by observing whether it is within an acceptable range or not. If it is beyond a widely adopted bound, this estimate must be rejected and a different solution such as the JTV solution may be adopted.

After the PS has been estimated, the LM algorithm is then applied to the source bearing estimation for determining the azimuth/elevation angle. We call this approach as the propagation speed-estimated (PSE) solution, the detail of which is given in Appendix C.

One evident disadvantage of the JTV model is estimating the PS as a redundant variable; another drawback of this model is leading to a system matrix, which is likely to be ill-conditioned [28].

IV. MEASUREMENT-DIVISION MODEL AND CRLB

A. MEASUREMENT-DIVISION MODEL

The intuition behind our idea is division operation of the TDOA measurements available from an array. In doing so, two TDOA measurement equations are combined through a division to eliminate the PS parameter. In particular, for the original TDOA measurement equation

$$\mathbf{s}_\ell\mathbf{k} = \mathrm{c}\left(\hat{\tau}_\ell + \mathrm{n}_\ell\right), \quad \ell = 1, 2, \ldots N-1. \tag{9}$$

Let the J-th sensor be the benchmark for division. Dividing (9) for $\ell = \mathrm{i}$ ($\mathrm{i} \neq \mathrm{J}$) by (9) when $\ell = \mathrm{J}$ produces

$$\frac{\mathbf{s}_\mathrm{i}\mathbf{k}}{\mathbf{s}_\mathrm{J}\mathbf{k}} = \frac{\hat{\tau}_\mathrm{i} + \mathrm{n}_\mathrm{i}}{\hat{\tau}_\mathrm{J} + \mathrm{n}_\mathrm{J}}. \tag{10}$$

Generally there exists $\left|\hat{\tau}_\mathrm{J}\right| \gg \mathrm{n}_\mathrm{J}$, so that the division can be reasonably approximated by

$$\frac{\mathbf{s}_\mathrm{i}\mathbf{k}}{\mathbf{s}_\mathrm{J}\mathbf{k}} = \frac{\hat{\tau}_\mathrm{i}}{\hat{\tau}_\mathrm{J}} + \frac{\mathrm{n}_\mathrm{i}}{\hat{\tau}_\mathrm{J}}. \tag{11}$$

It can be reshaped by

$$\mathrm{n}_\mathrm{i} = \frac{\hat{\tau}_\mathrm{J}\mathbf{s}_\mathrm{i}\mathbf{k}}{\mathbf{s}_\mathrm{J}\mathbf{k}} - \hat{\tau}_\mathrm{i}, \quad \mathrm{i} = 1, 2, \ldots, N-1;\ \mathrm{i} \neq \mathrm{J}, \tag{12}$$

which is rewritten in matrix-form to be

$$\mathbf{n} = \frac{\hat{\tau}_\mathrm{J}\mathbf{S}\mathbf{k}}{\mathbf{s}_\mathrm{J}\mathbf{k}} - \hat{\boldsymbol{\tau}}. \tag{13}$$

Such a division transform leads to a new speed-free error equation, which can be deemed as a pseudo-measurement equation different from the original one. When the covariance matrix of $\mathbf{n}$ is given by $\boldsymbol{\Sigma}$, the quadratic error function w.r.t. a hypothesized DOA is

$$\varepsilon\left(\boldsymbol{\gamma}\right) = \left(\frac{\hat{\tau}_\mathrm{J}\mathbf{S}\mathbf{k}}{\mathbf{s}_\mathrm{J}\mathbf{k}} - \hat{\tau}\right)^{\mathrm{T}} \boldsymbol{\Sigma}^{-1} \left(\frac{\hat{\tau}_\mathrm{J}\mathbf{S}\mathbf{k}}{\mathbf{s}_\mathrm{J}\mathbf{k}} - \hat{\boldsymbol{\tau}}\right). \tag{14}$$

It is worth mentioning that the PS would be time-varying or inequivalent for different assemblies of signal measurements [30]. With regard to a group of TDOAs currently measured by a short-baseline array, we can normally assume that the time of signal propagation from source to array would not be long. During the period of signal propagation, the PS is basically constant in a certain space range. Thus, the same PS of each sensor can be eliminated in the pseudo-measurement equation by the measurement-division model.

Remark 1: To satisfy the constraint $\left|\hat{\tau}_\mathrm{J}\right| \gg \mathrm{n}_\mathrm{J}$, a sensor with the largest absolute TDOA value in a group of measurements is selected as the benchmark for division. Additionally, when estimating the bearing of a source, the MD model requires at least four sensors to resolve, including the TDOA measurement reference sensor.

Remark 2: Note that if assumption $\left|\hat{\tau}_\mathrm{J}\right| \gg \mathrm{n}_\mathrm{J}$ does not hold, the above model may have a small systematic bias. Since an approximation is made for mathematical tractability, the corresponding estimation would not be optimal, even if we use the exhaustive grid-search technique to minimize the error function.

B. CRLB OF MEASUREMENT-DIVISION MODEL

In the following, we simply use CRLB($\boldsymbol{\gamma}$) to represent the lower bound of the MD model to simplify the notation unless ambiguity occurs. The CRLB($\boldsymbol{\gamma}$) is related with the speed-free equation in terms of the estimated parameters $\hat{\boldsymbol{\gamma}}$ by using the observed TDOA data and the sensor coordinates. Based on the speed-free TDOA noise vector in (13), the estimation variance of the source bearing in the CRLB($\boldsymbol{\gamma}$) will be different from the former two items in the conventional CRLB ($\boldsymbol{\Theta}$).

In other words, the CRLB($\boldsymbol{\gamma}$) denotes the minimum variance for any estimator that estimates the parameter vector $\boldsymbol{\gamma}$ from the TDOA measurements about the MD model. A similar CRLB has also been analyzed for the nonlinear time-of-arrival localization to be linearized in [31], where a linearized CRLB and the conventional CRLB from the original measurement equation are compared.

As mentioned above, since $\tau_\mathrm{i}/\tau_\mathrm{J} = \mathbf{s}_\mathrm{i}\mathbf{k}/\mathbf{s}_\mathrm{J}\mathbf{k}$, and $\hat{\tau}_\mathrm{i} = \tau_\mathrm{i} + \mathrm{n}_\mathrm{i}$, we have $\hat{\tau}_\mathrm{i} = \tau_\mathrm{J}\frac{\mathbf{s}_\mathrm{i}\mathbf{k}}{\mathbf{s}_\mathrm{J}\mathbf{k}} + \mathrm{n}_\mathrm{i}$, where the noise-free τ_J instead of $\hat{\tau}_\mathrm{J}$ is used for the lower bound analysis. Let $\mathrm{f}_\mathrm{i}(\boldsymbol{\gamma}) = \tau_\mathrm{J}\frac{\mathbf{s}_\mathrm{i}\mathbf{k}}{\mathbf{s}_\mathrm{J}\mathbf{k}}$ and $[\mathrm{f}(\boldsymbol{\gamma})]_\mathrm{i} = \mathrm{f}_\mathrm{i}(\boldsymbol{\gamma})$ ($\mathrm{i} = 1, \ldots, N-1$). Under the Gaussian noise assumption of TDOA with $|\boldsymbol{\Sigma}|$ being the determinant of the covariance matrix, the likelihood function of $\boldsymbol{\gamma}$ given the measurement vector $\hat{\boldsymbol{\tau}}$ is specified by

$$p\left(\hat{\boldsymbol{\tau}} \mid \boldsymbol{\gamma}\right) = \frac{1}{(2\pi)^{\frac{N-1}{2}}|\boldsymbol{\Sigma}|^{\frac{1}{2}}}\exp \times \left\{-\frac{1}{2}\left[\hat{\boldsymbol{\tau}} - \mathrm{f}(\boldsymbol{\gamma})\right]^{\mathrm{T}} \boldsymbol{\Sigma}^{-1}\left[\hat{\boldsymbol{\tau}} - \mathrm{f}(\boldsymbol{\gamma})\right]\right\}. \tag{15}$$

For an unbiased estimate $\hat{\boldsymbol{\gamma}}$ of $\boldsymbol{\gamma}$, the CRLB confines the following achievable error covariance

$$\mathrm{E}\left[(\boldsymbol{\gamma} - \hat{\boldsymbol{\gamma}})(\boldsymbol{\gamma} - \hat{\boldsymbol{\gamma}})^{\mathrm{T}}\right] \geq \mathbf{F}^{-1}(\boldsymbol{\gamma}) \triangleq \mathrm{CRLB}(\boldsymbol{\gamma}) \tag{16}$$

where $\mathbf{F}(\gamma)$ is the Fisher information matrix (FIM). Under the assumption of Gaussian measurement noise and the assumption that the noise covariance is independent of the parameter, the FIM is defined by

$$\mathbf{F}(\boldsymbol{\gamma}) = \left(\nabla_{\boldsymbol{\gamma}} \mathrm{f}(\boldsymbol{\gamma})\right)^{T} \boldsymbol{\Sigma}^{-1} \nabla_{\boldsymbol{\gamma}} \mathrm{f}(\boldsymbol{\gamma}) \tag{17}$$

where $\nabla_{\boldsymbol{\gamma}} \mathrm{f}(\boldsymbol{\gamma})$ is the Jacobian of $\mathrm{f}(\boldsymbol{\gamma})$ w.r.t. $\boldsymbol{\gamma}$. The lower bound of the covariance matrix in terms of the unknown vector $\boldsymbol{\gamma}$ is determined by

$$\begin{aligned} \mathrm{Cov}(\boldsymbol{\gamma}) &\geq -\mathrm{E}\left[\frac{\partial^2 \ln\left(p\left(\hat{\boldsymbol{\tau}} \mid \boldsymbol{\gamma}\right)\right)}{\partial \boldsymbol{\gamma} \partial \boldsymbol{\gamma}^{T}}\right]^{-1} \\ &= \begin{bmatrix} \frac{\partial \mathrm{f}(\boldsymbol{\gamma})^{\mathrm{T}}}{\partial \varphi} \boldsymbol{\Sigma}^{-1} \frac{\partial \mathrm{f}(\boldsymbol{\gamma})}{\partial \varphi} & \frac{\partial \mathrm{f}(\boldsymbol{\gamma})^{\mathrm{T}}}{\partial \varphi} \boldsymbol{\Sigma}^{-1} \frac{\partial \mathrm{f}(\boldsymbol{\gamma})}{\partial \theta} \\ \frac{\partial \mathrm{f}(\boldsymbol{\gamma})^{\mathrm{T}}}{\partial \theta} \boldsymbol{\Sigma}^{-1} \frac{\partial \mathrm{f}(\boldsymbol{\gamma})}{\partial \varphi} & \frac{\partial \mathrm{f}(\boldsymbol{\gamma})^{\mathrm{T}}}{\partial \theta} \boldsymbol{\Sigma}^{-1} \frac{\partial \mathrm{f}(\boldsymbol{\gamma})}{\partial \theta} \end{bmatrix}^{-1}, \end{aligned} \tag{18}$$

whose right side is exactly the inverse of FIM represented by $\mathbf{F}^{-1}(\boldsymbol{\gamma})$. For the sake of brevity, we define

$$\begin{cases} A_i = \mathrm{x_i}\cos\theta\sin\varphi - \mathrm{y_i}\cos\theta\cos\varphi, & (19a) \\ B_i = \mathrm{x_i}\sin\theta\cos\varphi + \mathrm{y_i}\sin\theta\sin\varphi - \mathrm{z_i}\cos\theta & (19b) \end{cases}$$

and

$$\begin{cases} A_J = \mathrm{x_J}\cos\theta\sin\varphi - \mathrm{y_J}\cos\theta\cos\varphi, & (20a) \\ B_J = \mathrm{x_J}\sin\theta\cos\varphi + \mathrm{y_J}\sin\theta\sin\varphi - \mathrm{z_J}\cos\theta. & (20b) \end{cases}$$

Given $\mathrm{c}\tau_{\mathrm{J}} = \mathbf{s_J k}, \mathrm{i} = 1, \ldots, N-1$, the negative partial derivatives are

$$\begin{cases} \left[\frac{\partial f(\boldsymbol{\gamma})}{\partial \varphi}\right]_{\mathrm{i}} = \frac{\mathrm{A_i s_J k} + \mathrm{A_J s_i k}}{\mathrm{c s_J k}}, & (21a) \\ \left[\frac{\partial f(\boldsymbol{\gamma})}{\partial \theta}\right]_{\mathrm{i}} = \frac{\mathrm{B_i s_J k} + \mathrm{B_J s_i k}}{\mathrm{c s_J k}}. & (21b) \end{cases}$$

Substituting (21) into (18) yields the CRLB. Note that the PS exists in the CRLB expression, although it is not seen in the MD model. When computing the CRLB, this parameter is treated as a constant.

Analytically comparing the CRLBs under the two models of JTV and MD is not tractable. We shall rely on numerical evaluations for them over a number of randomly generated geometries and the results will be presented in Section VI.

V. ESTIMATION SOLUTION AND THEORETICAL PERFORMANCE

A. ESTIMATION SOLUTION

It seems that a linear estimator may be obtained if we multiply both sides with $\mathbf{s_J k}$ to the MD formula in (11). In fact, this multiplication leads to the following equation after substituting $\mathrm{c}\tau_{\mathrm{J}} = \mathbf{s_J k}$ into the noise item

$$\frac{1}{c}\left(\mathbf{s}_{\mathrm{i}} - \frac{\hat{\tau}_{\mathrm{i}} \mathbf{s}_{\mathrm{J}}}{\hat{\tau}_{\mathrm{J}}}\right)\mathbf{k} = \mathrm{n_i}, \tag{22}$$

which would equal to zero for a noise-free measurement. There is no linear relation between the unknown vector $\mathbf{k}$ and the data vector $\hat{\tau}$ in the formulation. Hence, we can only use the nonlinear optimization technique by constructing an error cost function to realize the estimate of $\boldsymbol{\gamma}$, such that the estimation output is straightly the source bearing.

The MD model is resolved by the LM algorithm as follows. Let $\hat{\boldsymbol{\gamma}}_{\mathrm{v}}$ be the current estimate of v-th iteration. Define

$$\mathrm{f}_{\mathrm{i}}^{(\mathrm{v})}(\boldsymbol{\gamma}) = \hat{\tau}_{\mathrm{J}} \frac{\mathbf{s_i}\hat{\mathbf{k}}}{\mathbf{s_J}\hat{\mathbf{k}}}\bigg|_{\boldsymbol{\gamma}=\hat{\boldsymbol{\gamma}}_{\mathrm{v}}} \tag{23}$$

and

$$\begin{cases} \mathrm{g}_{\mathrm{i}}^{(\mathrm{v})} = \mathrm{f}_{\mathrm{i}}^{(\mathrm{v})}(\boldsymbol{\gamma}) - \hat{\tau}_{\mathrm{i}}, \quad \mathrm{i} = 1, \ldots, N-1, & (24a) \\ \mathbf{g} = [\mathrm{g}_1, \ldots, \mathrm{g}_{N-1}]^{\mathrm{T}}. & (24b) \end{cases}$$

Determine the gradient of current DOA estimate as

$$\begin{cases} \mathrm{a}_{\mathrm{i},1} = \frac{\partial \mathrm{f}_{\mathrm{i}}^{(\mathrm{v})}(\boldsymbol{\gamma})}{\partial \varphi}\Big|_{\boldsymbol{\gamma}=\hat{\boldsymbol{\gamma}}_{\mathrm{v}}}, & (25a) \\ \mathrm{a}_{\mathrm{i},2} = \frac{\partial \mathrm{f}_{\mathrm{i}}^{(\mathrm{v})}(\boldsymbol{\gamma})}{\partial \theta}\Big|_{\boldsymbol{\gamma}=\hat{\boldsymbol{\gamma}}_{\mathrm{v}}}, & (25b) \\ [\mathbf{A}]_{\mathrm{i,j}} = \mathrm{a}_{\mathrm{i,j}}, \quad \mathrm{i} = 1, \ldots, N-1, \ \mathrm{j} = 1, 2. & (25c) \end{cases}$$

Symbolize λ as the nonnegative damping factor being adjusted at each iteration, and calculate the bearing increment vector by using

$$\boldsymbol{\delta} = \left(\mathbf{A}^{\mathrm{T}} \boldsymbol{\Sigma}^{-1} \mathbf{A} + \lambda \mathbf{I}\right)^{-1} \mathbf{A}^{\mathrm{T}} \boldsymbol{\Sigma}^{-1} \mathbf{g}. \tag{26}$$

Assume that the subscript v and $v+1$ respectively represents the vectors at the v-th and $(v+1)$-th iteration, and u stands for the correction factor, we check the new cost function $\mathbf{g}_{\mathrm{v}+1}^{\mathrm{T}} \boldsymbol{\Sigma}^{-1} \mathbf{g}_{\mathrm{v}+1}$ after each iteration. If the following condition is satisfied:

$$\mathbf{g}_{\mathrm{v}+1}^{\mathrm{T}} \boldsymbol{\Sigma}^{-1} \mathbf{g}_{\mathrm{v}+1} \geq \mathbf{g}_{\mathrm{v}}^{\mathrm{T}} \boldsymbol{\Sigma}^{-1} \mathbf{g}_{\mathrm{v}} + \mathbf{u}\left(\mathbf{A}_{\mathrm{v}}^{\mathrm{T}} \boldsymbol{\Sigma}^{-1} \mathbf{g}_{\mathrm{v}}\right)^{\mathrm{T}} \boldsymbol{\delta}_{\mathrm{v}}, \tag{27}$$

then the damping factor is increased by $\lambda_{\mathrm{v}+1} = \lambda_{\mathrm{v}} \mathrm{h}$, where h is the amplification factor greater than one, and the bearing increment vector is renewed. Otherwise, the damping factor is decreased by $\lambda_{\mathrm{v}+1} = \lambda_{\mathrm{v}}/\mathrm{h}$, and then

$$\hat{\boldsymbol{\gamma}}_{\mathrm{v}+1} = \hat{\boldsymbol{\gamma}}_{\mathrm{v}} + \boldsymbol{\delta}_{\mathrm{v}}. \tag{28}$$

The updated damping factor is used to modify the increment vector, and the bearing estimate is updated accordingly. The procedure continues until the bearing increment is sufficiently small. If the procedure fails to converge, we may resort to the initial guess as an estimate to make the result stable. According to the convention of the LM algorithm, those factors can be chosen as follows: $\lambda = 2$, $\mathrm{u} = 0.4$, and $\mathrm{h} = 1.5$. A detailed procedure of the estimation solution is shown in Table 1.

B. THEORETICAL PERFORMANCE EVALUATION

This section will give the theoretical estimation performance of the above solution by perturbation analysis. For the cost function to be minimized:

$$\varepsilon(\boldsymbol{\gamma}) = \mathbf{n}^{\mathrm{T}} \boldsymbol{\Sigma}^{-1} \mathbf{n}, \tag{29}$$

TABLE 1. Source bearing estimation procedure by using the Levenberg-Marquardt algorithm for the measurement-division model.

Input: sensor locations $(\mathbf{S})$, TDOA measurements $(\hat{\boldsymbol{\tau}})$, noise covariance matrix $(\boldsymbol{\Sigma})$, amplification factor (h), damping factor (λ), correction factor (u), iteration precision, and maximum iteration number.
Output: $\hat{\boldsymbol{\gamma}} = [\hat{\varphi},\ \hat{\theta}]^{\mathrm{T}}$
1: Apply the LLS estimator in [16] to estimate initial bearing as $\hat{\boldsymbol{\gamma}}_0$; set iterative number $\mathrm{i} = 0$
2: Calculate current $\mathrm{f}(\boldsymbol{\gamma})$ in (23), $\mathbf{g}$ in (24) and cost function by using $\mathbf{g}^{\mathrm{T}}\boldsymbol{\Sigma}^{-1}\mathbf{g}$
3: Determine current gradient $\mathbf{A}$ in (25)
4: Calculate gradient of cost function by using $\mathbf{A}^{\mathrm{T}}\boldsymbol{\Sigma}^{-1}\mathbf{g}$
5: Estimate bearing increment $\boldsymbol{\delta}$ in (26)
6: Update $\hat{\boldsymbol{\gamma}} \leftarrow \hat{\boldsymbol{\gamma}} + \boldsymbol{\delta}$. If termination qualification does not satisfy iteration precision, go to Step 7. Otherwise, go to Step 9 when maximum iteration number is achieved; go to Step 10 when not.
7: If (27) is satisfied, then $\lambda \leftarrow \lambda\mathrm{h}$ and go to Step 5; otherwise, $\lambda \leftarrow \lambda/\mathrm{h}$ and go to Step 8
8: Update $\mathrm{i} \leftarrow \mathrm{i}+1$, and go to Step 2
9: Take initial guess in Step 1 as current estimate
10: Output current bearing estimation as a result

we expand it in the Taylor series at the current parameter estimate $\hat{\boldsymbol{\gamma}}$ and retaining the first three terms, i.e. up to the second-order term. Accordingly,

$$\varepsilon\left(\hat{\boldsymbol{\gamma}}+\boldsymbol{\delta}\right) \approx \varepsilon\left(\hat{\boldsymbol{\gamma}}\right) + \left(\nabla^{\varepsilon}_{\hat{\boldsymbol{\gamma}}}\right)^{\mathrm{T}}\boldsymbol{\delta} + \frac{1}{2}\boldsymbol{\delta}^{\mathrm{T}}\mathbf{H}\left(\hat{\boldsymbol{\gamma}}\right)\boldsymbol{\delta} \tag{30}$$

where $\boldsymbol{\delta}$ is the bearing increment vector, $\nabla^{\varepsilon}_{\hat{\boldsymbol{\gamma}}}$ is a gradient vector of $\varepsilon(\boldsymbol{\gamma})$ w.r.t. $\boldsymbol{\gamma}$ at $\hat{\boldsymbol{\gamma}}$, and $\mathbf{H}\left(\hat{\boldsymbol{\gamma}}\right)$ is the Hessian of the cost function. Minimization of the right-hand side of (30) yields

$$\boldsymbol{\delta} = -\mathbf{H}^{-1}\left(\hat{\boldsymbol{\gamma}}\right)\nabla^{\varepsilon}_{\hat{\boldsymbol{\gamma}}}. \tag{31}$$

If $\mathbf{H}\left(\hat{\boldsymbol{\gamma}}\right)$ is sufficiently smooth at $\hat{\boldsymbol{\gamma}} = \boldsymbol{\gamma}$, we can obtain [32]

$$\mathbf{H}\left(\hat{\boldsymbol{\gamma}}\right) \approx \mathrm{E}\left[\mathbf{H}\left(\hat{\boldsymbol{\gamma}}\right)\right]. \tag{32}$$

Let $\nabla^{\varepsilon}_{\boldsymbol{\gamma}}$ be the gradient vector of $\varepsilon(\hat{\boldsymbol{\gamma}})$ at $\hat{\boldsymbol{\gamma}} = \boldsymbol{\gamma}$. We have

$$\nabla^{\varepsilon}_{\boldsymbol{\gamma}} = 2\left[\sum\nolimits_{\mathrm{i}=1}^{N-1}\frac{\partial \mathrm{n_i}}{\partial\varphi}\mathrm{n_i} \quad \sum\nolimits_{\mathrm{i}=1}^{N-1}\frac{\partial \mathrm{n_i}}{\partial\theta}\mathrm{n_i}\right]^{\mathrm{T}}. \tag{33}$$

If the value of $\mathrm{n_i}$ is small, then $\mathrm{E}\left\{\sum_{\mathrm{i}=1}^{N-1}\mathrm{n_i}\right\} = 0$. Therefore, there exists $\mathrm{E}\left\{\nabla^{\varepsilon}_{\boldsymbol{\gamma}}\right\} = \mathbf{0}$, where $\mathbf{0}$ is a zero vector. The estimation bias is determined by

$$\begin{aligned}\mathrm{Bias}\left(\hat{\boldsymbol{\gamma}}\right) &= \mathrm{E}\left(\hat{\boldsymbol{\gamma}}-\boldsymbol{\gamma}\right) \approx -\mathrm{E}\left[\mathbf{H}^{-1}\left(\boldsymbol{\gamma}\right)\nabla^{\varepsilon}_{\boldsymbol{\gamma}}\right] \\ &= -\mathrm{E}\left[\mathbf{H}^{-1}\left(\boldsymbol{\gamma}\right)\right]\mathrm{E}(\nabla^{\varepsilon}_{\boldsymbol{\gamma}}) = -\mathbf{H}^{-1}\left(\boldsymbol{\gamma}\right)\cdot\mathbf{0} = \mathbf{0}.\end{aligned} \tag{34}$$

It means that our solution to minimize $\varepsilon(\boldsymbol{\gamma})$ is approximately unbiased. The estimation covariance is derived from (31) to be

$$\mathrm{Cov}(\boldsymbol{\delta}) = \mathbf{H}^{-1}\left(\hat{\boldsymbol{\gamma}}\right)\mathrm{E}[\nabla^{\varepsilon}_{\hat{\boldsymbol{\gamma}}}(\nabla^{\varepsilon}_{\hat{\boldsymbol{\gamma}}})^{\mathrm{T}}]\mathbf{H}^{-1}\left(\hat{\boldsymbol{\gamma}}\right). \tag{35}$$

Supposing that $\nabla^{\mathbf{n}}_{\hat{\boldsymbol{\gamma}}}$ stands for the gradient vector of TDOA noises w.r.t.$\hat{\boldsymbol{\gamma}}$, there exist the following relations in the LM algorithm [17]:

$$\begin{cases} \boldsymbol{H}\left(\hat{\boldsymbol{\gamma}}\right) = 2(\nabla^{\mathbf{n}}_{\hat{\boldsymbol{\gamma}}})^{\mathrm{T}}\boldsymbol{\Sigma}^{-1}\nabla^{\mathbf{n}}_{\hat{\boldsymbol{\gamma}}}, & \text{(36a)} \\ \nabla^{\varepsilon}_{\hat{\boldsymbol{\gamma}}} = 2(\nabla^{\mathbf{n}}_{\hat{\boldsymbol{\gamma}}})^{\mathrm{T}}\boldsymbol{\Sigma}^{-1}\mathbf{n}, & \text{(36b)} \\ \mathrm{E}\left(\mathbf{n}\mathbf{n}^{\mathrm{T}}\right) = \boldsymbol{\Sigma}. & \text{(36c)} \end{cases}$$

Substituting (36) into (35) and taking some algebra manipulations, it is easy to obtain that

$$\mathrm{Cov}(\boldsymbol{\delta}) = \left[(\nabla^{\mathbf{n}}_{\hat{\boldsymbol{\gamma}}})^{\mathrm{T}}\boldsymbol{\Sigma}^{-1}\nabla^{\mathbf{n}}_{\hat{\boldsymbol{\gamma}}}\right]^{-1}. \tag{37}$$

For $\mathrm{f_i}(\boldsymbol{\gamma}) = \tau_{\mathrm{J}}\frac{\mathbf{s_i k}}{\mathbf{s_J k}}$ and $[\mathrm{f}(\boldsymbol{\gamma})]_{\mathrm{i}} = \mathrm{f_i}(\boldsymbol{\gamma})$ $(\mathrm{i} = 1, \ldots, N-1)$, when $\hat{\tau}_{\mathrm{J}}$ approximates to τ_{J}, there exists $\nabla^{\mathbf{n}}_{\hat{\boldsymbol{\gamma}}} = \nabla_{\boldsymbol{\gamma}}\mathrm{f}(\boldsymbol{\gamma})$. As a result, the inverse of FIM in (17) is identical to the covariance in (37). The mean square error of lowest possible bearing estimation equals variance if an estimator is unbiased. Because our estimation is unbiased as suggested above, it can be concluded that the resolving solution of the MD model approximatively reaches the CRLB of this model.

In principle, the CRLB can be attained when the following constraints are satisfied. These constraints are: 1) the quantity of Hessian matrix is small, or the quantity of cost function is small; 2) Hessian matrix is sufficiently smooth around the true value; and 3) the final estimation error is small. We derive the bias and covariance of the proposed solution under the three constraints.

Remark 3: As we cannot obtain the uncorrupted τ_J and only replace it with the measurement $\hat{\tau}_J$, an error caused by approximation would exist. However, the estimation performance of our solution would be close to CRLB in general, which will be validated by the following simulations. Although the proposed method is not optimal, its estimation accuracy can still make it promising when confronted with an unknown PS.

VI. SIMULATION EVALUATION

In this section, four simulation examples are used to evaluate the performance of the proposed model and solution. Simulation assumptions are made below.

(1) Five sensors are deployed to form an array for simulation unless stated otherwise. The x-axis and y-axis coordinates of sensor locations are randomly selected within a ring of 30 m radius, while the z-axis coordinates are randomly selected in the smaller range [-5 m, 5 m], which simulates the typical situation of a ground-based array in practice.

(2) The TDOA measurement error is assumed as Gaussian noise with a specific standard deviation (STD). The TDOA STDs range from 0 ms to 3 ms, considering the propagation of air acoustic signal in simulation. We generate the TDOA noise variables of a group of measurement from an array, by using multivariate normal random numbers and adopting the simplified covariance matrix as mentioned earlier.

(3) Each simulation is conducted over 50 000 Monte Carlo trials. The iteration precision is set as 10^{-5} for those methods with an iterative operation. The estimation result of LLS is employed as the first guess for iteration to verify practicability in all iterative solutions.

(4) When the geometrical relation between source bearing and array coordinates is very unfavorable for DOA estimation, such as the source is located at one end of a linear array, the corresponding estimate would seriously deteriorate the statistic results. We have used a measure that when the absolute error of azimuth or elevation from the CRLB based on the JTV model exceeds 90°, we abandon the simulated generated geometrical structure of source and array this time, and replace it with another one.

(5) The estimated azimuth and elevation should usually be within the bound $[0, 2\pi]$ and $[-\pi/2, \pi/2]$, respectively. If the azimuth and elevation estimate correspondingly exceeds a multiple of 2π and π, then modulo operation is taken into account to avoid the anomalous estimates in the rational angular space.

Example 1: (RMSE and Computation Complexity of Related Methods Under Random Source Bearings): The purpose of this example is to examine the performance difference among the LLS, the MD, the JTV and the PSE. We select the four solutions to be compared in the sense that all of them belong to a bearing estimator with an unknown PS parameter. The LLS method proposed in [16] is closed-form; while the MD, the JTV and the PSE are iterative solutions. The later three methods are given in IV. A section, Appendix B and Appendix C of this paper, respectively. The source azimuth and elevation are uniformly taken from [15°, 75°] to represent random source bearings in 3-D space. The performance evaluation index is root mean squared error (RMSE) of bearing estimation. The estimation error is the difference between the estimated and the true bearing.

The RMSEs from various random geometries are computed for each solution, and the results versus TDOA STD are shown in Fig. 2. As can be observed, the MD solution has the best estimation performance of azimuth and elevation comparing with the other three solutions when the PS is unknown. The estimation accuracy of the MD solution is not only better than the closed-form solution, i.e. the LLS, but also superior to the other iterative solutions, i.e. the JTV and the PSE.

Moreover, the RMSE versus signal-to-noise ratio (SNR) is also evaluated. We define SNR as SNR $= 10\log(\frac{1}{2r^2\sigma_\tau^2})$, where r represents the source range to the array origin [13]. As the far-field source has a large ratio of source range to the array aperture, r is assumed to be in the bound [1000 m, 4000 m] such that the source signal can be approximately treated as a plane wave. The SNR changes from -20 dB to 10 dB in simulation; while the range and the bearing of a source are randomly selected within the associated bounds for each simulation run. Given the SNR and the source range, the TDOA STD is calculated by the SNR definition.

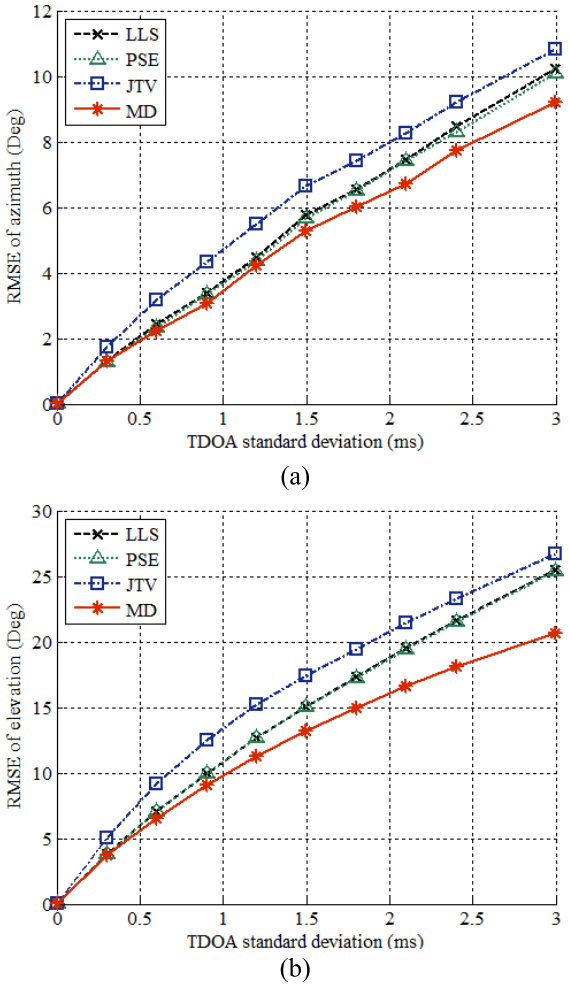

FIGURE 2. Angle estimation performance of the four estimators under random source bearings and random sensor locations versus different TDOA standard deviations. (a) Azimuth. (b) Elevation.

The other simulation parameters are determined in the same way. Given these parameters, the azimuth/elevation estimation is simulated under different SNRs. The performance of the bearing estimation in terms of RMSE versus SNR is shown in Fig. 3. It can be seen that the MD solution achieves the best performance, similar to the performance of RMSE versus TDOA STD. Thus, the MD solution is preferable among the different solutions.

Perhaps one disadvantage the MD solution has over the other solutions is the higher computation complexity. Table 2 shows the averaged computation time of the PSE, the JTV and the MD relative to that of the LLS. They are obtained from running the algorithms on a Laptop using Matlab codes and averaged over various TDOA STDs. Note that the absolute running time of the LLS is 17.68 μs. From the results we can observe that the time required by the MD is longer than those required by the LLS and the PSE, but still less than that of the JTV. Actually, the absolute time run by a modern electronic system would be rather short for

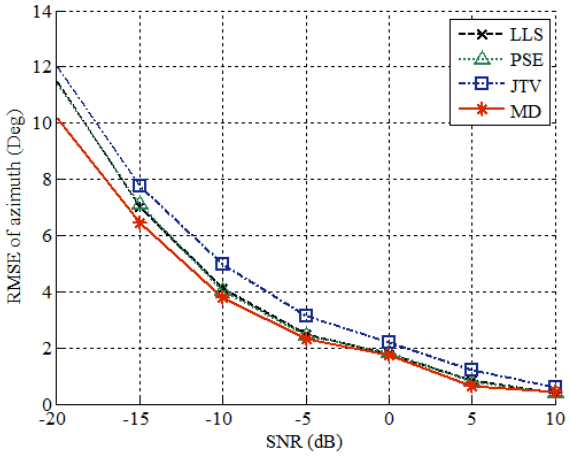

(a)

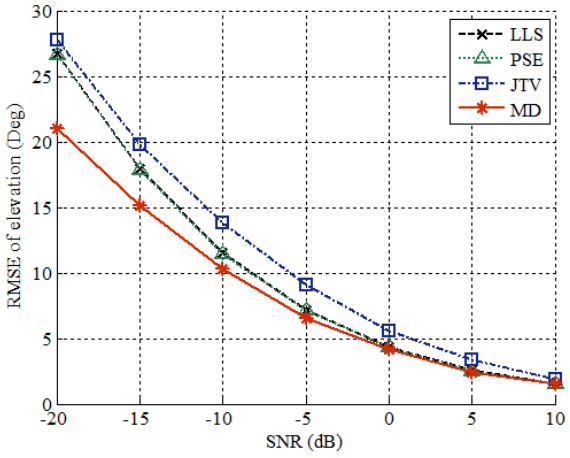

(b)

FIGURE 3. Angle estimation performance of the four estimators under random source bearings and random sensor locations versus different SNRs. (a) Azimuth. (b) Elevation.

TABLE 2. Relative averaged computation time of the four estimators involving LLS, PSE, JTV and MD. The results are averaged over a group of TDOA STDs identical to those in Fig. 2.

LLS	PSE	JTV	MD
1	6.83	22.94	19.52

these estimators to execute when the number of array sensors is not very large. Thus, the MD solution is preferable for a wide range of scenarios when both accuracy and computation efficiency are taken into account.

Example 2: (CRLB Comparison of Two Models): We compare the CRLB difference between the models of MD and JTV, denoted by MD-CRLB and JTV-CRLB respectively. The expressions of the two CRLBs have correspondingly been provided in IV. B section and Appendix A of the paper. The source azimuth and elevation are individually set as 45° and 15°. It represents the typical occasion of low-altitude source generally measured by a ground-based array. For different TDOA STDs, the theoretical RMSE of the two models

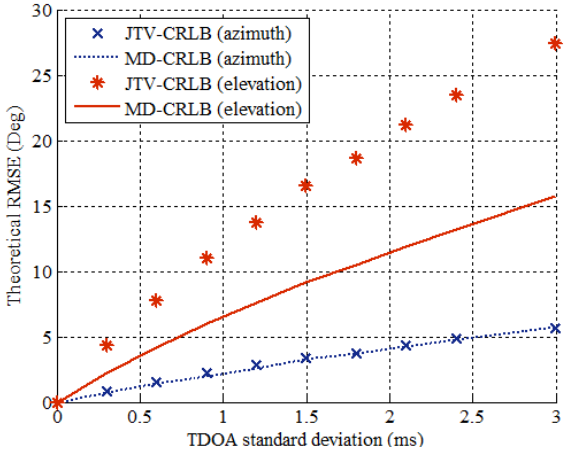

FIGURE 4. CRLBs of azimuth/elevation between the JTV model and the MD model versus different TDOA standard deviations.

are provided by Fig. 4. It is perceived that both of azimuth CRLBs are identical, while the MD-CRLB is much better than the JTV-CRLB in elevation.

We also verify the performance of the two CRLBs when the number of array sensors is different, ranging from four to ten. The simulation results are shown in Fig. 5, where the TDOA STD is fixed by 1.5 ms. Similar CRLB results to those with the fixed sensor number above can be observed, except when the number of sensors is the minimum (i.e. four), the JTV-CRLB has a little superiority. Overall the MD-CRLB is superior to the JTV-CRLB.

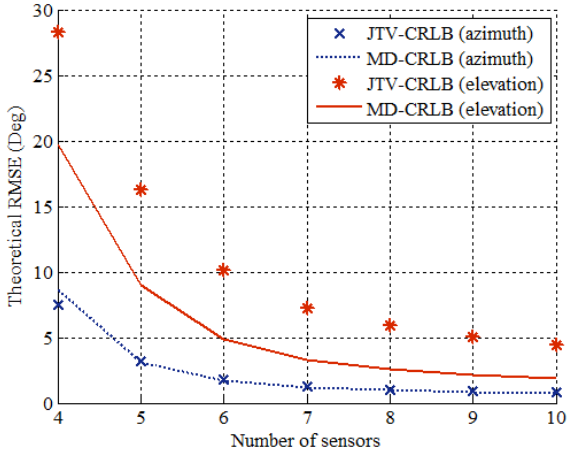

FIGURE 5. CRLBs of azimuth/elevation between the JTV model and the MD model versus different number of sensors.

Example 3: (Estimation Error of the MD Solution): This example is used to observe the estimation performance of the MD solution in comparison to the MD-CRLB. The simulation parameters are identical to the data in Example 2. The RMSEs of azimuth and elevation are provided in Fig. 6, and accompanied with the corresponding MD-CRLB. We can find from the figure that the RMSEs of the solution are close to the CRLBs, especially for the azimuth estimation.

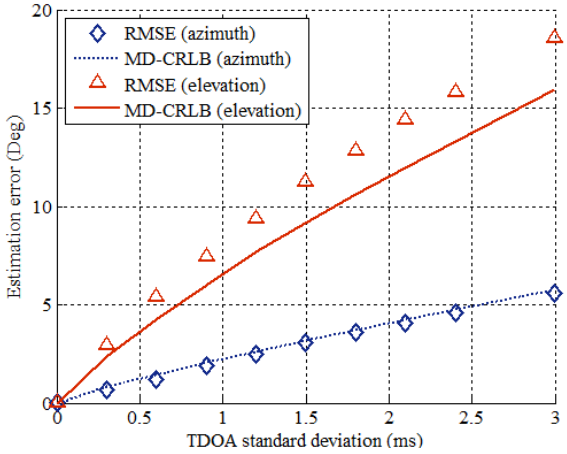

FIGURE 6. Estimation error of azimuth/elevation between the MD solution and the CRLBs versus different TDOA standard deviations.

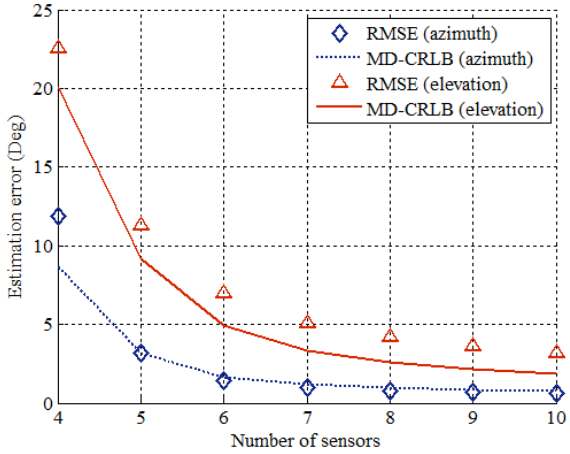

FIGURE 7. Estimation error of azimuth/elevation between the MD solution and the CRLBs versus different number of sensors.

In the case of different number of array sensors, the estimation errors of the MD solution are provided in Fig. 7. Similar to the results in Fig. 6, the RMSEs in this figure almost approach the corresponding MD-CRLBs. The example suggests that the MD solution can perform well in the source bearing estimation for various conditions.

Example 4: (Iterative Number of the MD Solution): The iterative number reflects the running efficiency of an iterative method. The example calculates the numbers of the MD solution under random geometries when they are converged. The required iterations are plotted using "boxplot" as illustrated in Fig. 8. The box top and bottom edge is the 25th and 75th percentile on every box, respectively. The box top whisker extending to the most extreme data points represents the maximum statistical generation not considered outliers, which are denoted by red crosses.

It is seen that the MD solution can converge after about 10 iterative steps for all TDOA STDs. The maximum number of iterations is smaller than 30, if not considering those outliers. These results show that the MD solution has a good convergence rate, and can run rapidly with manageable complexity.

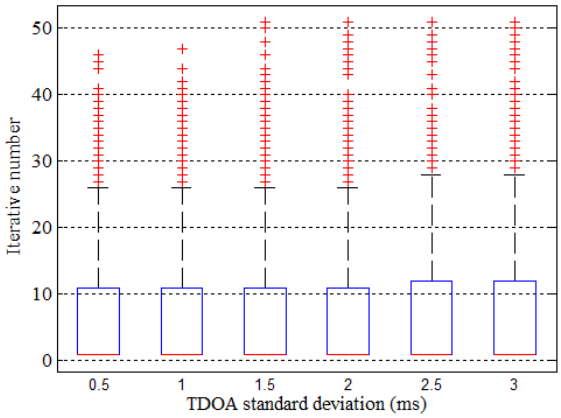

FIGURE 8. Boxplot of iterative number versus different TDOA standard deviations, where the MD solution is converged over the 50 000 randomly generated geometries.

VII. CONCLUSION

In practice, the wave speed of a source signal is usually unknown and varies considerably with the environment. This paper proposed a speed-free model and the associated solution to estimate the source bearing by using the TDOA measurements, with particular attention on the situations where a precise PS is unavailable. The significance of this work is that the source bearing estimation can still be accurately accomplished without the knowledge of PS. This is due to that we have reformulated the original TDOA measurement model to exclude the speed parameter by a division formulation. An iterative nonlinear solution has been developed to obtain the estimate of source bearing based on the proposed model. The model and solution have been evaluated by simulations. The results have demonstrated that the MD model has a superior CRLB to the JTV model, and the MD solution can outperform the existing methods with a practical running efficiency.

APPENDIX A
CRLB OF JOINT THREE-VARIABLE

Define $\mathrm{f_i}(\boldsymbol{\Theta}) = \mathbf{s_i k}/\mathrm{c}$, and $[\mathbf{f}(\boldsymbol{\Theta})]_\mathrm{i} = \mathrm{f_i}(\boldsymbol{\Theta}), \mathrm{i} = 1, \ldots, N-1$. For an unbiased estimator, the variance of the m-th element of $\boldsymbol{\Theta}$, namely $\boldsymbol{\Theta}(m)$ (m = 1, 2, 3), can be bounded by the CRLB

$$\mathrm{E}\left[\left(\hat{\boldsymbol{\Theta}}\,(\mathrm{m}) - \boldsymbol{\Theta}(\mathrm{m})\right)^2\right] \geq \mathrm{CRLB}\,(\boldsymbol{\Theta}\,(\mathrm{m}))\,. \qquad \text{(A.1)}$$

The conditional probability density function of TDOA measurement errors is described as

$$p\left(\hat{\boldsymbol{\tau}} \mid \boldsymbol{\Theta}\right) = \frac{1}{(2\pi)^{\frac{N-1}{2}} |\boldsymbol{\Sigma}|^{\frac{1}{2}}} \exp\left\{-\frac{1}{2}\left[\hat{\boldsymbol{\tau}} - \mathrm{f}(\boldsymbol{\Theta})\right]^{\mathrm{T}} \boldsymbol{\Sigma}^{-1}\left[\hat{\boldsymbol{\tau}} - \mathrm{f}(\boldsymbol{\Theta})\right]\right\}. \qquad \text{(A.2)}$$

For the unbiased estimate $\hat{\boldsymbol{\Theta}}$ of $\boldsymbol{\Theta}$, the corresponding CRLB and FIM is denoted by CRLB$(\boldsymbol{\Theta})$ and F$(\boldsymbol{\Theta})$, respectively. When the Jacobian of f$(\boldsymbol{\Theta})$ w.r.t. $\boldsymbol{\Theta}$ is given by ∇_{Θ}f$(\boldsymbol{\Theta})$, the FIM is expressed to be

$$\mathbf{F}(\boldsymbol{\Theta}) = (\nabla_{\Theta}\mathrm{f}(\boldsymbol{\Theta}))^{\mathrm{T}}\,\boldsymbol{\Sigma}^{-1}\nabla_{\Theta}\mathrm{f}(\boldsymbol{\Theta}). \tag{A.3}$$

Then the CRLB of the unknown vector $\boldsymbol{\Theta}$ is determined by (A.4), as shown at the bottom of this page, whose right side is $\mathbf{F}^{-1}(\boldsymbol{\Theta})$. The m-th parameter in the CRLB of the unknown vector $\boldsymbol{\Theta}$ is found by

$$\mathrm{CRLB}\left(\boldsymbol{\Theta}(\mathrm{m})\right) = \left[\mathbf{F}^{-1}(\boldsymbol{\Theta})\right]_{\mathrm{m,m}}. \tag{A.5}$$

For $\mathrm{i} = 1, \ldots, N-1$, the negative partial derivatives of f$(\boldsymbol{\Theta})$ are derived as

$$\begin{cases} \left[\dfrac{\partial f(\boldsymbol{\Theta})}{\partial \varphi}\right]_{\mathrm{i}} = \dfrac{\mathrm{x_i cos}\theta\mathrm{sin}\varphi - \mathrm{y_i cos}\theta\mathrm{cos}\varphi}{c}, & \text{(A.6a)} \\ \left[\dfrac{\partial f(\boldsymbol{\Theta})}{\partial \theta}\right]_{\mathrm{i}} = \dfrac{\mathrm{x_i sin}\theta\mathrm{cos}\varphi + \mathrm{y_i sin}\theta\mathrm{sin}\varphi - \mathrm{z_i cos}\theta}{c}, & \text{(A.6b)} \\ \left[\dfrac{\partial f(\boldsymbol{\Theta})}{\partial c}\right]_{\mathrm{i}} = \dfrac{\mathrm{x_i cos}\theta\mathrm{cos}\varphi + \mathrm{y_i cos}\theta\mathrm{sin}\varphi + \mathrm{z_i sin}\theta}{c^2}. & \text{(A.6c)} \end{cases}$$

After substituting these partial derivatives into (A.4), the CRLB about the JTV model can be determined.

APPENDIX B
SOLUTION OF JOINT THREE-VARIABLE

In the JTV solution, the quadratic error function of a hypothesized DOA and PS becomes

$$\varepsilon(\boldsymbol{\Theta}) = \left(\frac{\mathbf{Sk}}{c} - \hat{\boldsymbol{\tau}}\right)^{\mathrm{T}} \boldsymbol{\Sigma}^{-1} \left(\frac{\mathbf{Sk}}{c} - \hat{\boldsymbol{\tau}}\right). \tag{B.1}$$

With regard to the current variable estimate $\hat{\boldsymbol{\Theta}}_{\mathrm{v}}$ of v-th iteration, we have

$$\mathrm{f_i^{(v)}}(\boldsymbol{\Theta}) = \left.\frac{\mathbf{s_i}\hat{\mathbf{k}}}{\hat{\mathrm{c}}}\right|_{\boldsymbol{\Theta}=\hat{\boldsymbol{\Theta}}_{\mathrm{v}}} \tag{B.2}$$

and

$$\begin{cases} \mathrm{h_i^{(v)}} = \mathrm{f_i^{(v)}}(\boldsymbol{\Theta}) - \hat{\boldsymbol{\tau}}_{\mathrm{i}}, \quad \mathrm{i} = 1, \ldots, N-1, & \text{(B.3a)} \\ \mathbf{h} = [\mathrm{h}_1, \ldots, \mathrm{h}_{N-1}]^{\mathrm{T}}. & \text{(B.3b)} \end{cases}$$

The gradient of current estimate is

$$\begin{cases} \mathrm{b_{i,1}} = \left.\dfrac{\partial \mathrm{f_i^{(V)}}(\boldsymbol{\Theta})}{\partial \varphi}\right|_{\boldsymbol{\Theta}=\widehat{\boldsymbol{\Theta}}_{\mathrm{v}}}, & \text{(B.4a)} \\ \mathrm{b_{i,2}} = \left.\dfrac{\partial \mathrm{f_i^{(v)}}(\boldsymbol{\Theta})}{\partial \theta}\right|_{\boldsymbol{\Theta}=\widehat{\boldsymbol{\Theta}}_{\mathrm{v}}}, & \text{(B.4b)} \\ \mathrm{b_{i,3}} = \left.\dfrac{\partial \mathrm{f_i^{(v)}}(\boldsymbol{\Theta})}{\partial \mathrm{c}}\right|_{\boldsymbol{\Theta}=\widehat{\boldsymbol{\Theta}}_{\mathrm{v}}}, & \text{(B.4c)} \\ [\mathbf{B}]_{\mathrm{ij}} = \mathrm{b_{i,j}}, \quad \mathrm{i} = 1, \ldots, N-1, \quad \mathrm{j} = 1, 2, 3. & \text{(B.4d)} \end{cases}$$

The partial derivatives of f$(\boldsymbol{\Theta})$ has been given in (A.6). Then the bearing increment vector is calculated by

$$\boldsymbol{\delta} = (\mathbf{B}^{\mathrm{T}}\boldsymbol{\Sigma}^{-1}\mathbf{B} + \lambda\mathbf{I})^{-1}\mathbf{B}^{\mathrm{T}}\boldsymbol{\Sigma}^{-1}\mathbf{h}. \tag{B.5}$$

Similarly, the condition is examined as follows

$$\mathbf{h}_{\mathrm{v+1}}^{\mathrm{T}}\boldsymbol{\Sigma}^{-1}\mathbf{h}_{\mathrm{v+1}} \geq \mathbf{h}_{\mathrm{v}}^{\mathrm{T}}\boldsymbol{\Sigma}^{-1}\mathbf{h}_{\mathrm{v}} + \mathrm{u}\left(\mathbf{B}_{\mathrm{v}}^{\mathrm{T}}\boldsymbol{\Sigma}^{-1}\mathbf{h}_{\mathrm{v}}\right)^{\mathrm{T}}\boldsymbol{\delta}_{\mathrm{v}}. \tag{B.6}$$

The other operations are identical with those of the MD solution as mentioned above.

APPENDIX C
SOLUTION OF PROPAGATION SPEED-ESTIMATED

This solution is similar to the detail in Appendix B, except that the PS parameter is estimated by (8) in advance. For the current DOA estimate $\hat{\boldsymbol{\gamma}}_{\mathrm{v}}$ of v-th iteration, we correspondingly have

$$\mathrm{f_i^{(v)}}(\boldsymbol{\gamma}) = \left.\frac{\mathbf{s_i}\hat{\mathbf{k}}}{\hat{\mathrm{c}}}\right|_{\boldsymbol{\gamma}=\hat{\boldsymbol{\gamma}}_{\mathrm{v}}} \tag{C.1}$$

and

$$\begin{cases} \mathrm{h_i^{(v)}} = \mathrm{f_i^{(v)}}(\boldsymbol{\gamma}) - \hat{\tau}_{\mathrm{i}}, \quad \mathrm{i} = 1, \ldots, N-1, & \text{(C.2a)} \\ \mathbf{h} = [\mathrm{h}_1, \ldots, \mathrm{h}_{N-1}]^{\mathrm{T}}. & \text{(C.2b)} \end{cases}$$

We determine the gradient of current DOA estimate as

$$\begin{cases} \mathrm{b_{i,1}} = \left.\dfrac{\partial \mathrm{f_i^{(v)}}(\boldsymbol{\gamma})}{\partial \varphi}\right|_{\boldsymbol{\gamma}=\hat{\boldsymbol{\gamma}}_{\mathrm{v}}}, & \text{(C.3a)} \\ \mathrm{b_{i,2}} = \left.\dfrac{\partial \mathrm{f_i^{(v)}}(\boldsymbol{\gamma})}{\partial \theta}\right|_{\mathrm{v}=\hat{\boldsymbol{\gamma}}_{\mathrm{v}}}, & \text{(C.3b)} \\ [\mathbf{B}]_{\mathbf{i,j}} = \mathrm{b_{i,j}}, \quad \mathrm{i} = 1, \ldots, N-1, \quad \mathrm{j} = 1, 2. & \text{(C.3c)} \end{cases}$$

$$\mathrm{Cov}(\boldsymbol{\Theta}) \geq -\mathbf{E}\left[\frac{\partial^2 \ln\left(p\left(\hat{\boldsymbol{\tau}} \mid \boldsymbol{\Theta}\right)\right)}{\partial\boldsymbol{\Theta}\partial\boldsymbol{\Theta}^{T}}\right]^{-1} = \begin{bmatrix} \frac{\partial \mathrm{f}(\boldsymbol{\Theta})^{\mathrm{T}}}{\partial\varphi}\boldsymbol{\Sigma}^{-1}\frac{\partial \mathrm{f}(\boldsymbol{\Theta})}{\partial\boldsymbol{\varphi}} & \frac{\partial \mathrm{f}(\boldsymbol{\Theta})^{\mathrm{T}}}{\partial\varphi}\boldsymbol{\Sigma}^{-1}\frac{\partial \mathrm{f}(\boldsymbol{\Theta})}{\partial\theta} & \frac{\partial \mathrm{f}(\boldsymbol{\Theta})^{\mathrm{T}}}{\partial\varphi}\boldsymbol{\Sigma}^{-1}\frac{\partial \mathrm{f}(\boldsymbol{\Theta})}{\partial c} \\ \frac{\partial \mathrm{f}(\boldsymbol{\Theta})^{\mathrm{T}}}{\partial\theta}\boldsymbol{\Sigma}^{-1}\frac{\partial \mathrm{f}(\boldsymbol{\Theta})}{\partial\varphi} & \frac{\partial \mathrm{f}(\boldsymbol{\Theta})^{\mathrm{T}}}{\partial\theta}\boldsymbol{\Sigma}^{-1}\frac{\partial \mathrm{f}(\boldsymbol{\Theta})}{\partial\theta} & \frac{\partial \mathrm{f}(\boldsymbol{\Theta})^{\mathrm{T}}}{\partial\theta}\boldsymbol{\Sigma}^{-1}\frac{\partial \mathrm{f}(\boldsymbol{\Theta})}{\partial c} \\ \frac{\partial \mathrm{f}(\boldsymbol{\Theta})^{\mathrm{T}}}{\partial c}\boldsymbol{\Sigma}^{-1}\frac{\partial \mathrm{f}(\boldsymbol{\Theta})}{\partial\varphi} & \frac{\partial \mathrm{f}(\boldsymbol{\Theta})^{\mathrm{T}}}{\partial c}\boldsymbol{\Sigma}^{-1}\frac{\partial \mathrm{f}(\boldsymbol{\Theta})}{\partial\theta} & \frac{\partial \mathrm{f}(\boldsymbol{\Theta})^{\mathrm{T}}}{\partial c}\boldsymbol{\Sigma}^{-1}\frac{\partial \mathrm{f}(\boldsymbol{\Theta})}{\partial c} \end{bmatrix}^{-1} \tag{A.4}$$

The remaining procedure is the same as that of the JTV solution.

ACKNOWLEDGMENT

The authors would like to thank the anonymous reviewers for improving the clarity and quality of the paper.

REFERENCES

[1] M. Burtowy, M. Rzymowski, and L. Kulas, "Low-profile ESPAR antenna for RSS-based DoA estimation in IoT applications," *IEEE Access*, vol. 7, pp. 17403–17411, 2019.

[2] Y. Wang and K. C. Ho, "TDOA positioning irrespective of source range," *IEEE Trans. Signal Process.*, vol. 65, no. 6, pp. 1447–1460, Mar. 2017.

[3] M. M. Rabik and T. Muthuramalingam, "Tracking and locking system for shooter with sensory noise cancellation," *IEEE Sensors J.*, vol. 18, no. 2, pp. 732–735, Jan. 2018.

[4] K. Yu, R. E. Hudson, Y. D. Zhang, K. Yao, C. Taylor, and Z. Wang, "Low-complexity 2D direction-of-arrival estimation for acoustic sensor arrays," *IEEE Signal Process. Lett.*, vol. 23, no. 12, pp. 1791–1795, Dec. 2016.

[5] X. Zhang, T. Jiang, Y. Li, and X. Liu, "An off-grid DOA estimation method using proximal splitting and successive nonconvex sparsity approximation," *IEEE Access*, vol. 7, pp. 66764–66773, 2019.

[6] K. Aghababaiyan, R. G. Zefreh, and V. Shah-Mansouri, "3D-OMP and 3D-FOMP algorithms for DOA estimation," *Phys. Commun.*, vol. 31, pp. 87–95, Dec. 2018.

[7] J. Dmochowski, J. Benesty, and S. Affes, "Direction of arrival estimation using the parameterized spatial correlation matrix," *IEEE Trans. Audio, Speech, Lang. Process.*, vol. 15, no. 4, pp. 1327–1339, May 2007.

[8] P. Annibale, J. Filos, P. A. Naylor, and R. Rabenstein, "TDOA-based speed of sound estimation for air temperature and room geometry inference," *IEEE Trans. Audio, Speech, Language Process.*, vol. 21, no. 2, pp. 234–246, Feb. 2013.

[9] X. Cui, K. Yu, and S. Lu, "Evolutionary TDOA-based direction finding methods with 3-D acoustic array," *IEEE Trans. Instrum. Meas.*, vol. 64, no. 9, pp. 2347–2359, Sep. 2015.

[10] R. Bahroun, O. Michel, F. Frassati, M. Carmona, and J. L. Lacoume, "New algorithm for footstep localization using seismic sensors in an indoor environment," *J. Sound Vib.*, vol. 333, no. 3, pp. 1046–1066, Feb. 2014.

[11] P. Annibale, "Direct propagation speed estimation for delay-based acoustic applications," Ph.D. dissertation, Dept. Multimedia Commun. Signal Process., Univ. Erlangen-Nuremberg, Erlangen, Germany, Dec. 2014.

[12] R. Rabenstein and P. Annibale, "Acoustic source localization under variable speed of sound conditions," *Wireless Commun. Mobile Comput.*, vol. 2017, Oct. 2017, Art. no. 9524943, doi: 10.1155/2017/9524943.

[13] X. Cui, K. Yu, and S. Lu, "TDOA-based acoustic direction finding," in *Positioning and Navigation in Complex Environments*, K. Yu, Ed. Hershey, PA, USA: IGI Global, Jan. 2018, pp. 193–232.

[14] J.-A. Luo, X.-P. Zhang, Z. Wang, and X.-P. Lai, "On the accuracy of passive source localization using acoustic sensor array networks," *IEEE Sensors J.*, vol. 17, no. 6, pp. 1795–1808, Mar. 2017.

[15] R. K. Martin, A. S. King, J. R. Pennington, R. W. Thomas, R. Lenahan, and C. Lawyer, "Modeling and mitigating noise and nuisance parameters in received signal strength positioning," *IEEE Trans. Signal Process.*, vol. 60, no. 10, pp. 5451–5463, Oct. 2012.

[16] B. Berdugo, M. A. Doron, J. Rosenhouse, and H. Azhari, "On direction finding of an emitting source from time delays," *J. Acoust. Soc. Amer.*, vol. 105, no. 6, pp. 3355–3363, Jun. 1999.

[17] D. W. Marquardt, "An algorithm for least-squares estimation of nonlinear parameters," *J. Soc. Ind. Appl. Math.*, vol. 11, no. 2, pp. 431–441, Jun. 1963.

[18] R. Poisel, *Electronic Warfare Target Location Methods*, 2nd ed. London, U.K.: Artech House, 2012.

[19] X. Qu, L. Xie, and W. Tan, "Iterative constrained weighted least squares source localization using TDOA and FDOA measurements," *IEEE Trans. Signal Process.*, vol. 65, no. 15, pp. 3990–4003, May 2017.

[20] Y. T. Chan and K. C. Ho, "A simple and efficient estimator for hyperbolic location," *IEEE Trans. Signal Process.*, vol. 42, no. 8, pp. 1905–1915, Aug. 1994.

[21] L. Rui and K. C. Ho, "Efficient closed-form estimators for multistatic sonar localization," *IEEE Trans. Aerosp. Electron. Syst.*, vol. 51, no. 1, pp. 600–614, Jan. 2015.

[22] M. Dehghani and K. Aghababaiyan, "FOMP algorithm for direction of arrival estimation," *Phys. Commun.*, vol. 26, pp. 170–174, Feb. 2018.

[23] C. W. Reed, R. Hudson, and K. Yao, "Direct joint source localization and propagation speed estimation," in *Proc. IEEE Int. Conf. Acoust., Speech, Signal Process. (ICASSP)*, Phoenix, AZ, USA, vol. 3, Mar. 1999, pp. 1169–1172.

[24] A. Mahajan and M. Walworth, "3D position sensing using the differences in the time-of-flights from a wave source to various receivers," *IEEE Trans. Robot. Autom.*, vol. 17, no. 1, pp. 91–94, Feb. 2001.

[25] J. Zheng, K. W. Lui, and H.-C. So, "Accurate three-step algorithm for joint source position and propagation speed estimation," *Signal Process.*, vol. 87, no. 12, pp. 3096–3100, Dec. 2007.

[26] R. Diamant and L. Lampe, "Underwater localization with time-synchronization and propagation speed uncertainties," *IEEE Trans. Mobile Comput.*, vol. 12, no. 7, pp. 1257–1269, Jul. 2013.

[27] K. W. K. Lui, W.-K. Ma, H. C. So, and F. K. W. Chan, "Semi-definite programming algorithms for sensor network node localization with uncertainties in anchor positions and/or propagation speed," *IEEE Trans. Signal Process.*, vol. 57, no. 2, pp. 752–763, Feb. 2009.

[28] J.-S. Hu and C.-H. Yang, "Estimation of sound source number and directions under a multisource reverberant environment," *EURASIP J. Adv. Signal Process.*, vol. 2010, no. 1, pp. 1–14, 2010, doi: 10.1155/2010/870756.

[29] X. Cui, K. Yu, and S. Lu, "Approximate closed-form TDOA-based estimator for acoustic direction finding via constrained optimization," *IEEE Sensors J.*, vol. 18, no. 8, pp. 3360–3371, Apr. 2018.

[30] J. Han, S. P. Chepuri, Q. Zhang, and G. Leus, "Iterative per-vector equalization for orthogonal signal-division multiplexing over time-varying underwater acoustic channels," *IEEE J. Ocean. Eng.*, vol. 44, no. 1, pp. 240–255, Jan. 2019.

[31] P.-H. Tseng and K.-T. Feng, "Geometry-assisted localization algorithms for wireless networks," *IEEE Trans. Mobile Comput.*, vol. 12, no. 4, pp. 774–789, Apr. 2013.

[32] H. C. So, Y. T. Chen, K. C. Ho, and Y. Chen, "Simple formulae for bias and mean square error computation [DSP tips and tricks]," *IEEE Signal Process. Mag.*, vol. 30, no. 4, pp. 162–165, Jul. 2013.

XUNXUE CUI received the B.S. degree in artillery and the M.S. degree in operation research from Hefei Artillery Academy, Hefei, China, in 1991 and 1996, respectively, and the Ph.D. degree in pattern recognition and artificial intelligence from the University of Science and Technology of China, Hefei, in 2001. He served as a Postdoctoral Fellow with the Department of Computer Science and Technology, Tsinghua University, Beijing, China, from 2002 to 2004. He is currently a Distinguished Professor with the School of Electrical and Information Engineering, Anhui University of Science and Technology, China. He has published some regular articles in the IEEE Transactions/Journal as the first author. His research interests include signal processing, direction finding, and target localization (particularly for acoustic source). He is a member of the China Computer Federation Technical Committee on the Internet of Things.

KEGEN YU (SM'12) received the Ph.D. degree in electrical engineering from the University of Sydney, Sydney, NSW, Australia, in 2003.

He was with Jiangxi Geological and Mineral Bureau, Nanchang, China, Nanchang University, Nanchang, China, the University of Oulu, Oulu, Finland, the CSIRO ICT Center, Sydney, NSW, Australia, Macquarie University, Sydney, the University of New South Wales, Sydney, and Wuhan University, Wuhan, China. He is currently a Distinguished Professor with the School of Environmental Science and Spatial Informatics, China University of Mining and Technology, Xuzhou, China. He has coauthored the books: *Ground-Based Wireless Positioning* (Wiley and IEEE Press, 2009, a Chinese version of the book is also available) and *Wireless Positioning: Principles and Practice* (Springer, 2018), and has authored or coauthored more than 130 refereed journal and conference papers. He has edited the books: *Positioning and Navigation in Complex Environments* (IGI Global, 2018) and *Indoor Positioning and Navigation* (Science Press, 2019). His research interests include global-navigation-satellite-system reflectometry, ground-based and satellite-based positioning, and remote sensing.

Dr. Yu was a recipient of the Hundred Talent Program of Hubei Province and granted the Honor of Hubei Distinguished Expert, in 2015. He served on the editorial boards of the *EURASIP Journal on Advances in Signal Processing*, the IEEE TRANSACTIONS ON AEROSPACE AND ELECTRONIC SYSTEMS, and the IEEE TRANSACTIONS ON VEHICULAR TECHNOLOGY, from 2013 to 2017. He was the Lead Guest Editor for a Special Issue of the Physical Communication on Indoor Navigation and Tracking and for a Special Issue of the *EURASIP Journal on Advances in Signal Processing* on GNSS remote sensing.

BAITING ZHAO received the Ph.D. degree in control science and engineering from the Harbin Institute of Technology, in 2010. He is currently an Associate Professor with the School of Electrical and Information Engineering, Anhui University of Science and Technology, China. His research interests include image processing and intelligent control.